# Thermal Diffusion Effect On Dissipative Fluid Flow Past A Vertical Porous Plate In Presence Of Transverse Magnetic Field

B. Rajesh and K. Sarada*

*Department of Mathematics, RGUKT (APIIIT - Nuzvid), Nuzvid, Krishna (Dt), 521202, Andhra Pradesh State, India.*

*Department of Mathematics, Government City College, Nayapul, Hyderabad, Telangana State, India.*

**Abstract:** In this paper, the influence of thermal diffusion (Soret) on electrically conducting, incompressible, viscous dissipative fluid flow past an oscillating vertical plate in presence of transverse magnetic field, heat and mass transfer is studied. The basic governing equations representing the physical model is a system of partial differential equations which are transformed into systems of coupled linear partial differential equations by introducing non-dimensional variables. The resulting equations are solved using finite element method. The computational results for velocity, temperature and the concentration profiles are displayed graphically for various flow pertinent parameters. The result shows that an increase in Eckert number of the fluid actually increases the velocity and temperature profiles of the flow, whereas an increase in thermal diffusion parameter rises the velocity and concentration distributions.

***Keywords:*** Thermal diffusion; Viscous dissipation; MHD; Porous Medium; Finite element method;

## Nomenclature:

**List of variables:**

| | |
|---|---|
| $k_1$ | Permeability of the fluid |
| $u'$ | The velocity of the fluid in $x'$ – direction |
| $H(t')$ | Unit step function $(s)$ |
| $U$ | Constant velocity at the plate ($m\ s^{-1}$) |
| $x'$ | Coordinate axis along the plate ($m$) |
| $y'$ | Co-ordinate axis normal to the plate ($m$) |
| $T'$ | Fluid Temperature $(K)$ |
| $C_p$ | Specific heat at constant pressure |
| $t'$ | Time $(s)$ |
| $B_0$ | Uniform magnetic field (*Tesla*) |
| $T'_\infty$ | Fluid temperature away from the plate |
| $T'_w$ | Fluid temperature at the wall $(K)$ |
| $C'$ | Species concentration ($Kg\ m^{-3}$) |
| $i$ | Unit vector in the vertical flow direction |
| $C'_w$ | Concentration of the plate ($Kg\ m^{-3}$) |
| $C'_\infty$ | Concentration of the fluid far away from the plate ($Kg\ m^{-3}$) |
| $Gc$ | Grashof number for mass transfer |
| $u$ | Non dimensional fluid velocity ($m\ s^{-1}$) |
| $t$ | Non dimensional time $(s)$ |
| $Sh$ | The local Sherwood number |
| $Gr$ | Grashof number for heat transfer |
| $M$ | Magnetic field parameter |
| $D_m$ | Mass diffusivity ($m^2\ s^{-1}$) |
| $T_m$ | Mean fluid temperature $(K)$ |
| $K$ | Permeability parameter |
| $D$ | Solute mass diffusivity ($m^2\ s^{-1}$) |
| $Nu$ | The local Nusselt number |
| $C_f$ | The local skin-friction ($N\ m^{-2}$) |
| $g$ | Acceleration due to gravity, 9.81 ($m\ s^{-2}$) |
| $y$ | Dimensionless displacement ($m$) |
| $Sr$ | Soret number |
| $Ec$ | Eckert number |
| $\Pr$ | Prandtl number |
| $Sc$ | Schmidt number |
| $k_T$ | Thermal diffusion ratio |

**Greek Symbols:**

| | |
|---|---|
| $\tau'$ | Stress tensor of Casson fluid ($N\ m^{-2}$) |
| $\rho$ | The constant density $(kg\,m^{-3})$ |
| $\beta$ | Volumetric coefficient of thermal expansion ($K^{-1}$) |
| $\beta^*$ | Volumetric Coefficient of thermal expansion with concentration ($m^3\ Kg^{-1}$) |
| $\kappa$ | Thermal conductivity of the fluid |
| $\sigma$ | Electric conductivity of the fluid $(s\ m^{-1})$ |
| $\varphi$ | Porosity |
| $\omega'$ | Dimensionless Frequency of oscillation of the plate ($m\ s^{-1}$) |
| $\phi$ | Fluid Concentration ($Kg\ m^{-3}$) |
| $\theta$ | Fluid temperature $(K)$ |

$\omega$ Frequency of oscillation of the plate

$\tau$ Stress tensor of Casson fluid $(N\ m^{-2})$

$\nu$ Kinematic viscosity $(m^2\ s^{-1})$

**Subscripts:**

$'$ Dimensionless Properties

**Superscripts:**

$w$ Conditions on the wall

$\infty$ Free stream conditions

$p$ Plate

# 1. Introduction:

The study of combined heat and mass transfer has taken much attention to researchers because of its paramount applications in engineering and technology such as air cooler, nuclear reactor, heat generation, nuclear safety, design of industrial equipment, paper making, chemical catalytic reactor, etc. Recently, the several researchers focused on rotating vertical cone due to its numerous applications mainly engineering and technology, geophysical, design of turbo machine, design of spacecrafts etc. In view of these applications, Tien [1] illustrated the convective laminar heat transfer about a rotating cone. Alamgir [2] developed the approximate solution of steady two-dimensional heat transfer through a vertical cone with laminar convection. Chand et al. [3] reported free convective Darcian flow through a truncated cone. Pop and Takhar [4] describes the influence of compressibility in laminar natural convection flow over a vertical cone. Takhar et al [5] described the effect of magnetic field on variable mixed convection flow past a rotating vertical cone. Sandeep and Sulochana [6] analyzed unsteady mixed convection flow over a stretching surface. Palani and Kim [7] determined the combined effects of magnetic field and thermal radiation on convective heat and mass transfer over a vertical cone. Mahdy et al. [8] describes the influence of magnetic field and thermal radiation on double diffusive convection towards a vertical cone in a saturated porous medium. Nadeem and Saleem [9] analytically studied the mixture of free and forced unsteady convection flow of a rotating nano fluid through a vertical cone. Mallikarjuna et al [10] analyzed the effect of chemical reaction on an unsteady MHD boundary layer convective heat and mass transfer flow over a circulating cone about a porous regime. The results of thermal radiation and heat source on an unsteady MHD free convective fluid flow over an infinite vertical plate in occurrence of thermal diffusion and diffusion thermo were discussed by Raju et al. [11]. Anand Rao et al. [12] demonstrated the combined effects of heat and mass transfer on unsteady MHD flow past a vertical oscillatory plate suction velocity using finite element method. Anand Rao et al. [13] studied transient flow past an impulsively started infinite flat porous plate in a rotating fluid in presence of magnetic field with Hall current using finite element technique. The combined effects of heat and mass transfer on unsteady MHD natural convective flow past an infinite vertical plate enclosed by porous medium in presence of thermal radiation and Hall Current was investigated by Ramana Murthy et al. [14]. Rao et al. [15] found the numerical results of the non-linear partial differential equations of free convective magnetohydrodynamic flow past semi-infinite moving vertical plate with the effects of thermal radiation and viscous dissipation using finite element technique. Srinivasa Raju [16] studied the combined effects of thermal-diffusion and diffusion-thermo on unsteady free convection fluid flow past an infinite vertical porous plate in presence of magnetic field and chemical reaction using finite element technique.

The motivation of this study is to investigate the influence of thermal diffusion and viscous dissipation on magnetohydrodynamic newtonian fluid over a vertical plate embedded in porous medium in presence of heat and mass transfer. The governing momentum, heat and mass transfer equations are, in general, strongly coupled and highly linear. The purpose of this study are (i) to investigate the effects of different physical parameters on the velocity, temperature, and concentration profiles of the problem, and (ii) to apply finite element method for solving highly coupled, linear system of partial differential equations.

# 2. Formulation of the Problem:

For this formulation of this problem, we made the following assumptions:

i. The flow being confined to $y' > 0$ where $y'$ is the coordinate measured in the normal direction to the plate.

ii. The fluid is assumed to be electrically conducting with a uniform magnetic field $B_0$ is applied in a direction perpendicular to the plate.

iii. The magnetic Reynolds number is assumed to be small enough to neglect the effects of induced magnetic field.

iv. Initially, for time $t'=0$, both the fluid and the plate are at rest with uniform temperature.

v. At the same time, the plate temperature is raised to $T'_w$ which is thereafter maintained constant and concentration is raised to $C'_w$ which is thereafter maintained constant.

vi. At time $t'=0$ the plate begins to oscillate in its plane $y'=0$ according to

$$V = UH(t')\cos(\omega' t')i \text{ ; or } V = U\sin(\omega' t')i \text{ at } t'>0 \tag{1}$$

Under the assumptions made above, the governing partial differential equations for the fully developed magnetohydrodynamic heat and mass transfer free convective heat and mass transfer flow are

*Momentum Equation:*

$$\frac{\partial u'}{\partial t'} = \nu \frac{\partial^2 u'}{\partial y'^2} - \sigma B_0^2 u' - \frac{\mu\varphi}{k_1} u' + \rho g \beta (T' - T'_\infty) + \rho g \beta (C' - C'_\infty) \tag{2}$$

*Energy Equation:*

$$\frac{\partial T'}{\partial t'} = \frac{\kappa}{\rho C_p} \frac{\partial^2 T'}{\partial y'^2} + \nu \left( \frac{\partial u'}{\partial y'} \right)^2 \tag{3}$$

*Species Diffusion Equation:*

$$\frac{\partial C'}{\partial t'} = D \frac{\partial^2 C'}{\partial y^2} + \frac{D_m k_T}{T_m} \frac{\partial^2 T'}{\partial y'^2} \tag{4}$$

together with initial and boundary conditions

$$\left. \begin{array}{l} t'<0: \quad u'=0, \quad T'=T'_\infty, \; C'=C'_\infty \text{ for all } y' \\ t'\geq 0: \begin{cases} u'=UH(t')\cos(\omega' t') \quad \text{or} \quad u'=u'\sin(\omega' t'), \quad T'=T'_w, \; C'=C'_w \text{ at } y'=0 \\ u'\to 0, \; T'\to T'_\infty, \; C'\to C'_\infty \quad \text{as} \quad y'\to\infty \end{cases} \end{array} \right\} \tag{5}$$

We introduce the following dimensionless variables

$$\left. \begin{array}{l} u=\dfrac{u'}{U}, \; y=\dfrac{y'U}{\nu}, t=\dfrac{U^2}{\nu}t', \theta=\dfrac{T'-T'_\infty}{T'_w-T'_\infty}, \; \phi=\dfrac{C'-C'_\infty}{C'_w-C'_\infty}, \; \omega=\dfrac{\omega'\nu}{U^2}, \tau=\dfrac{\tau'}{\rho u^2}, \; Sc=\dfrac{\nu}{D}, \\ M=\dfrac{\sigma B_0^2 \nu}{\rho U^2}, \; K=\dfrac{\nu\varphi^2}{k_1 U^2}, \; Gr=\dfrac{\nu g\beta(T'_w-T'_\infty)}{U^3}, \; \Pr=\dfrac{\nu\rho C_p}{\kappa}, \; Gc=\dfrac{\nu g\beta^*(C'_w-C'_\infty)}{U^3}, \\ Ec=\dfrac{\nu}{C_p(T'_w-T'_\infty)}, \; Sr=\dfrac{D_m k_T(T'_w-T'_\infty)}{\nu T_m(C'_w-C'_\infty)} \end{array} \right\} \tag{6}$$

Substituting the above non-dimensionless variables into Eqs. (2)-(4), and we get

$$\frac{\partial u}{\partial t} = \frac{\partial^2 u}{\partial y^2} - Mu - \frac{1}{K}u + Gr\theta + Gc\phi \tag{7}$$

$$\frac{\partial \theta}{\partial t} = \frac{1}{\Pr} \frac{\partial^2 \theta}{\partial y^2} + Ec \left( \frac{\partial u}{\partial y} \right)^2 \tag{8}$$

$$\frac{\partial \phi}{\partial t} = \frac{1}{Sc} \frac{\partial^2 \phi}{\partial y^2} + Sr \left( \frac{\partial^2 \theta}{\partial y^2} \right) \tag{9}$$

with associated initial and boundary conditions

$$\left.\begin{array}{l} t<0: u=0,\ \theta=0,\ \phi=0 \text{ for all } y \\ t\geq 0: \begin{cases} u=H(t)\cos(\omega t) \text{ or } u=\sin(\omega t),\ \theta=1,\ \phi=1 \text{ at } y=0 \\ u\to 0,\ \theta\to 0,\ \phi\to 0 \text{ as } y\to\infty \end{cases} \end{array}\right\} \tag{10}$$

The Skin-friction at the plate, which in the non-dimensional form is given by

$$Cf=\left(\frac{\tau'_w}{\rho U\nu}\right)=\left(\frac{\partial u}{\partial y}\right)_{y=0} \tag{11}$$

The rate of heat transfer coefficient in terms of the Nusselt number is given by

$$Nu=-x'\frac{\left(\dfrac{\partial T'}{\partial y'}\right)_{y'=0}}{T'_w-T'_\infty}\Rightarrow Nu\,\mathrm{Re}_x^{-1}=-\left(\frac{\partial\theta}{\partial y}\right)_{y=0} \tag{12}$$

The rate of mass transfer coefficient in terms of the Sherwood number, is given by

$$Sh=-x'\frac{\left(\dfrac{\partial C'}{\partial y'}\right)_{y'=0}}{C'_w-C'_\infty}\Rightarrow Sh\,\mathrm{Re}_x^{-1}=-\left(\frac{\partial\phi}{\partial y}\right)_{y=0} \tag{13}$$

## 3. Method of Solution by Finite Element Method:

**3.1. Finite Element Method (FEM):** The main feature of the FEM ([17] and [18]), able to explain the geometry of the problem being analyzed with high flexibility. This is because of the discretization of the problem domain is performed using with flexible elements or uniform or non uniform patches that can be simply depict complex shapes either regular or irregular. Essentially the method is consist continuously piecewise function for the solution and to obtain the parameters of the functions in a methodical way, that minimize the error in the solution. The following steps are involved in finite element analysis.

**3.1.1. Discretization of the Domain:** The fundamental concept of the FEM, the region or domain of the problem divided into tiny connected patches, called as finite elements. The collection of the elements is called as the finite element mesh. These finite elements are coupled in a non overlapping method, such that it covers the complete domain of the problem.

**3.1.2. Generation of the Element Equations:**

i) Isolated a typical element from the mesh, the various formulation of the problem is assembled over the typical element.

ii) Over an element, a fairly accurate solution of the variational problem is supposed, and by substituting this in the system, group of element equations will be generate.

iii) The element matrix is obtained by using the element interpolation functions; the element matrix is also called as a stiffness matrix.

**3.1.3. Assembly of the Element Equations:** Assemble the algebraic equations by applying the inter element continuity conditions. This yields gives so many algebraic equations, called as the global finite element model, which governs the entire region.

**3.1.4. Imposition of the Boundary Conditions:** The physical boundary conditions defined in (10) are applied in the assembled equations.

**3.1.5. Solution of Assembled Equations:** The assembled algebraic equations can be solved by numerical techniques, either direct or indirect methods, Such as LU decomposition, Gauss elimination, Jacobin, Seidal methods. For computational purposes, the $y$ coordinate is various from 0 to $y_{\max}$ = 3 where $y_{\max}$ represents the infinity $i.e.,$ external to the momentum, energy and concentration boundary layers. The entire domain is split into a group of 100 line segments with equal width 0.1 and each element being two-noded.

The entire domain or region is divided into 10000 linear elements with an equivalent size. Each element represents two-nodded, and the entire domain contains 20001 nodes. To be evaluating the three functions at each and every node. Hence, after assemble the element equations, we obtain a system of 80004 equations which are combination of linear and non-linear. The systems convert to linear by incorporating known function $\bar{u}$. Therefore, after applying the boundary conditions, a system of linear equations are obtained which are solved by an efficient Gauss elimination method with maintaining an accuracy of 0.00000001. A convergence criterion is based on the relative difference between the current and previous iterations. When that differences are satisfy the desired accuracy. The Gaussian quadrature is applied for evaluating the integrations. The code of the algorithm is executed in MATLAB. Excellent convergence results were achieved.

## 4. Results and Discussions

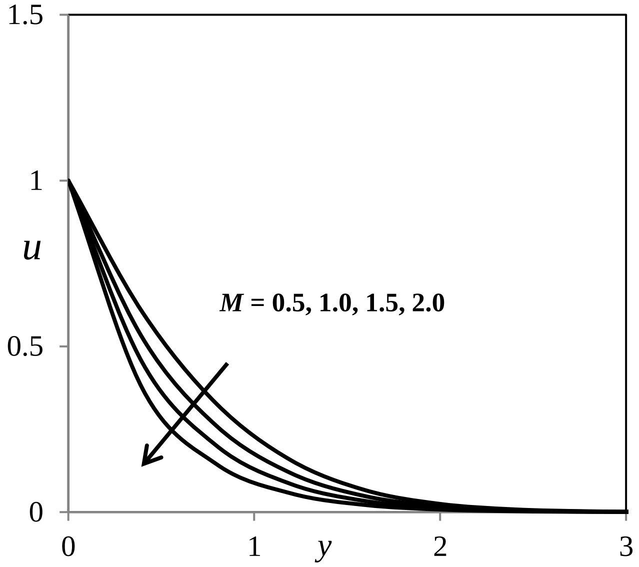


**Fig. 1.** Velocity profiles for various values of *M*

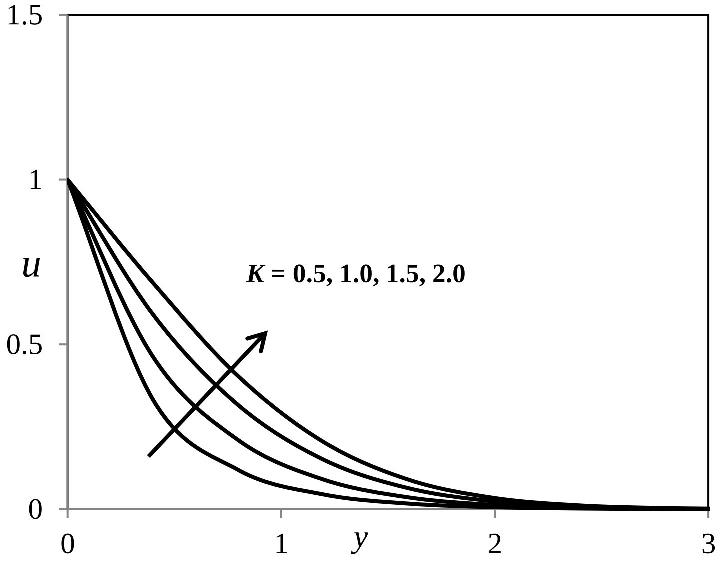


**Fig. 2.** Velocity profiles for various values of *K*

The influence of Magnetic field parameter on the velocity profile is shown in the. Fig. 1. It is observed that the fluid velocity decreases with increasing of Magnetic field parameter. As expected, because of the application of transverse magnetic field will result in a resistive type force (Lorentz force) similar to drag force which tends to resist the fluid flow and thus reducing its velocity. Also, the boundary layer thickness decreases with an increase of the Magnetic parameter. We also see that the fluid velocity decrease with the increase of magnetic effect indicating that magnetic field tends to retard the motion of the fluid.

Magnetic field may control the flow attributes. Fig. 2. Shows the velocity distribution with the influence of porous media parameter. The velocity is increasing with enhancement of the permeability parameter. The identical behavior is expected, because when we increase the permeability parameter, i.e. Increases the size of the pores inside the porous medium due to which the drag force decreases and hence the velocity increases.

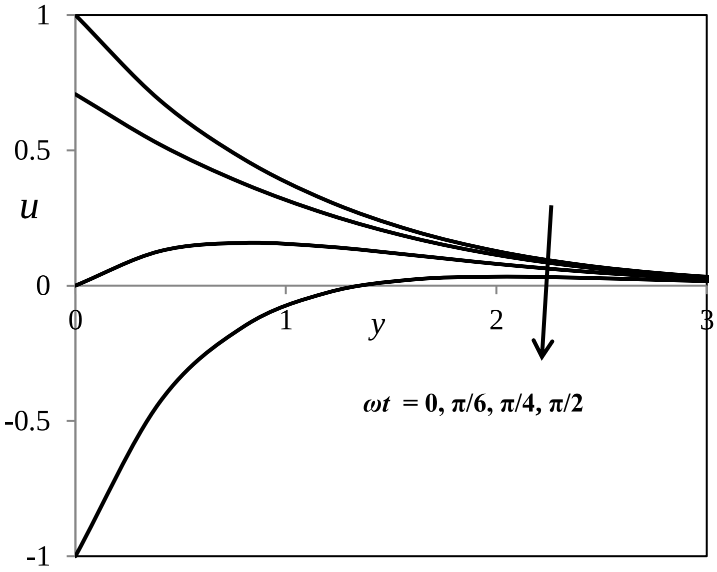


**Fig. 3.** Velocity profiles for various values of $\omega t$

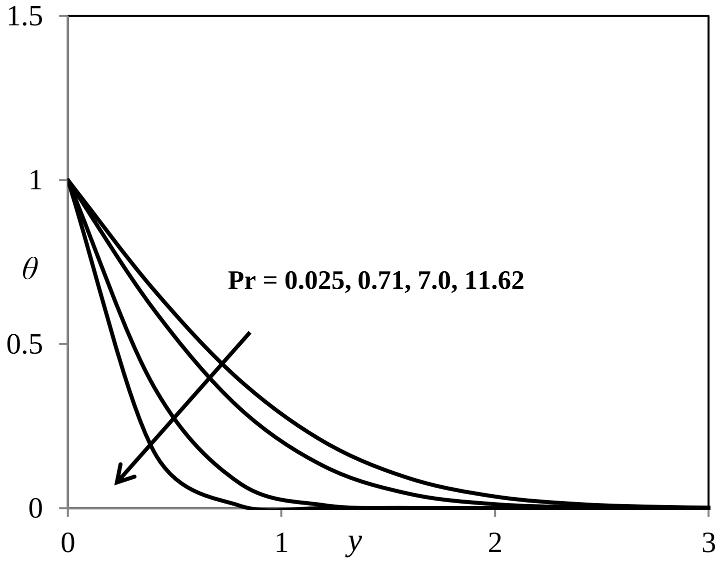


**Fig. 4.** Temperature profiles for various values of Pr

The velocity profiles for various values of phase angle $\omega t$ is illustrated in Fig. 3. It is found that the fluid velocity oscillating between -1 to 1 for any value of phase angle $\omega t$ at near the plate while asymptotically approaches to zero away from the plate (i. e. $y$ tends to infinity). Therefore the velocity shows an oscillatory behavior due to the sinusoidal boundary condition. Near the plate, the oscillations are of great significance. The temperature profiles are plotted in Fig. 4 for various values of the Prandtl number. The Prandtl number defines the ratio of momentum diffusivity to thermal diffusivity. From Fig. 4, it is clear that the fluid temperature decreases as increasing of Prandtl number, hence, thermal boundary layer thickness reduces as an increasing of Prandtl number. Figs. 5 and 6 show the velocity and temperature profiles with an influence of Eckert number respectively. The Eckert number is the ratio of the kinetic energy of the flow to the boundary layer enthalpy difference. The fluid temperature as well as the fluid velocity increases as increasing of Eckert number. Fig. 7 shows the concentration profile with an influence of Schmidt number.

Schmidt number is the ratio of viscous force of the fluid to chemical molecular diffusivity of the fluid. The fluid concentration decreases as increasing of Schmidt number due to molecular diffusion decreases. Figs. 8 and 9 shows the velocity and concentration distribution with an influence of Soret number respectively. Fluid velocity and concentration increases as increasing of temperature gradient. Since enhance the temperature gradient as increasing of Soret number.

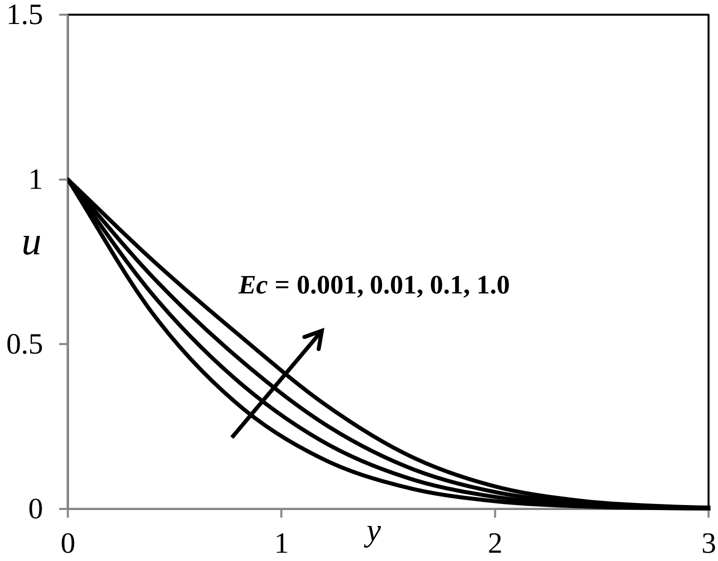


**Fig. 5.** Velocity profiles for various values of *Ec*

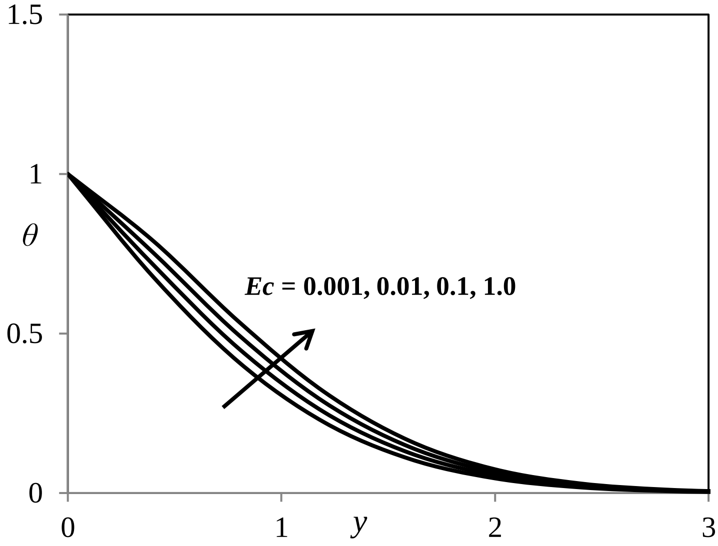


**Fig. 6.** Temperature profiles for various values of *Ec*

The numerical values of Skin-friction coefficient due to velocity profiles are presented in table-1 with the effects of Grashof number for heat transfer, Grashof number mass transfer, Porous medium parameter, Viscous dissipation parameter, Soret number, Prandtl number, Schmidt number, Magnetic field parameter and Phase angle parameter. From this table, we observed that, the Skin-friction coefficient is increased as increasing of Grashof number for heat transfer, Grashof number mass transfer, Porous medium parameter, Viscous dissipation parameter, Soret number and the reverse effect is observed as increasing of Prandtl number, Schmidt number, Magnetic field parameter and Phase angle parameter. The rate of heat transfer coefficient or Nusselt number coefficient due to temperature profiles are discussed using the numerical values in table-2. From this table we observed that, the rate of heat transfer increasing as increasing of Viscous dissipation parameter while decreases as increasing of Prandtl number. Also, from the same table we observed that the rate of mass transfer increasing as increasing of Schmidt number while decreases as increasing of Soret number.

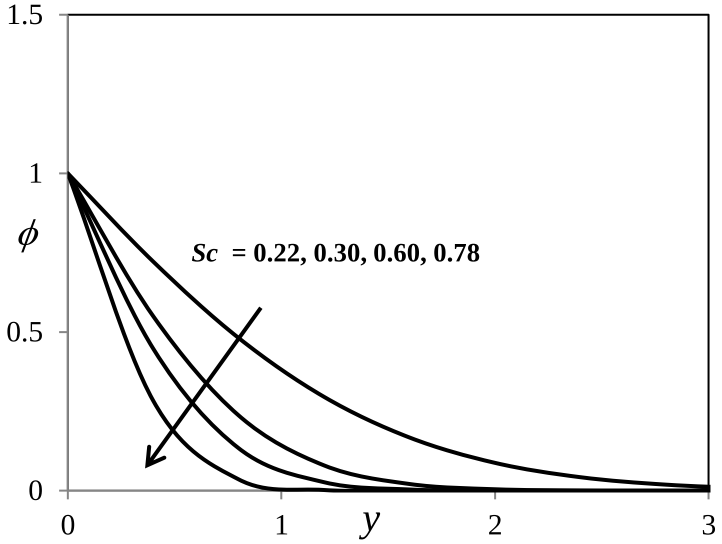


**Fig. 7.** Concentration profiles for various values of *Sc*

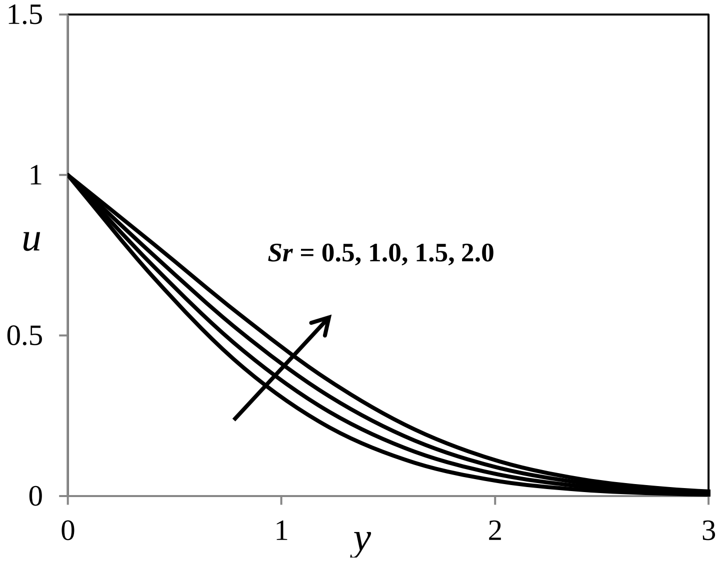


**Fig. 8.** Velocity profiles for various values of *Sr*

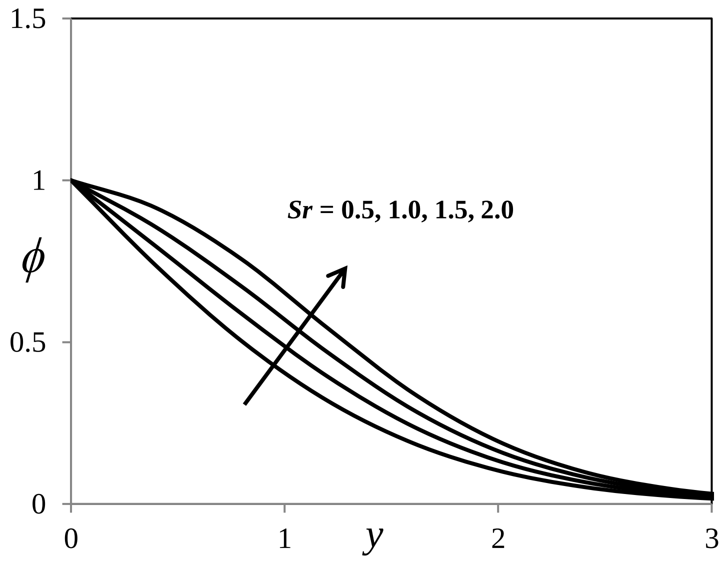


**Fig. 9.** Concentration profiles for various values of *Sr*

**Table-1:** The numerical values of Skin-friction coefficient due to velocity profiles

| *Gr* | *Gc* | *M* | Pr | *Sc* | *Ec* | *Sr* | *K* | *ωt* | *Cf* |
|---|---|---|---|---|---|---|---|---|---|
| 1.0 | 1.0 | 0.5 | 0.71 | 0.22 | 0.001 | 0.5 | 0.5 | π/4 | 1.3566215891 |
| **2.0** | 1.0 | 0.5 | 0.71 | 0.22 | 0.001 | 0.5 | 0.5 | π/4 | 1.4522177846 |
| 1.0 | **2.0** | 0.5 | 0.71 | 0.22 | 0.001 | 0.5 | 0.5 | π/4 | 1.4930047515 |
| 1.0 | 1.0 | **1.0** | 0.71 | 0.22 | 0.001 | 0.5 | 0.5 | π/4 | 1.2420156874 |
| 1.0 | 1.0 | 0.5 | **7.00** | 0.22 | 0.001 | 0.5 | 0.5 | π/4 | 1.2310066521 |
| 1.0 | 1.0 | 0.5 | 0.71 | **0.30** | 0.001 | 0.5 | 0.5 | π/4 | 1.2530691782 |
| 1.0 | 1.0 | 0.5 | 0.71 | 0.22 | **1.000** | 0.5 | 0.5 | π/4 | 1.3932647862 |
| 1.0 | 1.0 | 0.5 | 0.71 | 0.22 | 0.001 | **1.0** | 0.5 | π/4 | 1.4032157847 |
| 1.0 | 1.0 | 0.5 | 0.71 | 0.22 | 0.001 | 0.5 | **1.0** | π/4 | 1.3962447156 |
| 1.0 | 1.0 | 0.5 | 0.71 | 0.22 | 0.001 | 0.5 | 0.5 | **π/2** | 1.2762214881 |

**Table-2:** The numerical values of rate of heat and mass transfer coefficients

| Pr | *Ec* | *Nu* | *Sc* | *Sr* | *Sh* |
|---|---|---|---|---|---|
| 0.71 | 0.001 | 0.5122448625 | 0.22 | 0.5 | 0.5322695514 |
| **7.00** | 0.001 | 0.3650114785 | **0.30** | 0.5 | 0.3755120046 |
| 0.71 | **1.000** | 0.5581174521 | 0.22 | **1.0** | 0.6011487552 |

## 5. Conclusions:

The joint effects of thermal diffusion and viscous dissipation on unsteady magnetohydrodynamic free convective newtonian fluid flow past over an oscillating vertical plate embedded in porous medium in presence of heat and mass transfer is discussed. Finite element method is employed for basic equations of the flow with suitable oscillatory boundary conditions. From this research problem the following conclusions are made:

1. The fluid velocity increased as increasing of Porous medium parameter, Viscous dissipation parameter and Soret number while decreased as increasing of Magnetic field parameter and Phase angle parameter.
2. The fluid temperature increased as increasing of Viscous dissipation parameter while decreased as increasing of Prandtl number.
3. The fluid concentration is increased as increasing of Soret number while decreased as increasing of Schmidt number.
4. The Skin-friction coefficient is increased as increasing of Grashof number for heat transfer, Grashof number mass transfer, Porous medium parameter, Viscous dissipation parameter and Soret number while decreased as increasing of Prandtl number, Schmidt number, Magnetic field parameter and Phase angle parameter.
5. The rate of heat transfer increasing as increasing of Viscous dissipation parameter while decreases as increasing of Prandtl number.
6. The rate of mass transfer increasing as increasing of Schmidt number while decreases as increasing of Soret number.

## References:

1. C. L. Tien, Heat and mass transfer by laminar flow from a rotating cone, ASME J. Heat. Transf., 82 (1960), pp. 252-253.
2. M. Alamgir, Over-all heat transfer from vertical cone in laminar free convection: an approximate method, ASME J. Heat Transfer, 101 (1989) 174-176.
3. P. Cheng, T.T. Le, I. Pop, Natural convection of a Darcian fluid about a cone, Int. Commun. Heat. Mass Transf., 12 (1985), pp. 705-717.

4. I. Pop, H.S. Takhar, Compressibility effect in laminar free convection from a vertical cone, Appl. Sci. Res., 48 (1991), pp. 78-82.
5. H. S. Takhar, A. J. Chamkha, G. Nath, Unsteady mixed convection flow from a rotating vertical cone with magnetic field, Heat. Mass Transf., 39 (2003), pp. 297-304.
6. N. Sandeep, C. Sulochana, Dual solutions for unsteady mixed convection flow of MHD micropolar fluid over a stretching/shrinking sheet with non-uniform heat source/sink, Eng. Sci. Technol., Int. J., 18 (2015), pp. 738-745.
7. G. Palani, K.Y. Kim, Influence of magnetic field and thermal radiation by natural convection past vertical cone subjected to variable heat flux, Appl. Math. Mech. Engl., 33 (5) (2012), pp. 605-620.
8. A. Mahdy, A.J. Chamkha, Y. Baba, Double-diffusive convection with variable from a vertical truncated cone in porous media in the presence of magnetic field and radiation effects, Comput. Math. Appl., 59 (2010), pp. 3867-3878.
9. S. Nadeem, S. Saleem, Analytical study of rotating non-Newtonian nanofluid on a rotating cone, J. Thermophys. Heat. Transf., 28 (2) (2014), pp. 295-302.
10. B. Mallikarjuna, A.M. Rashad, A.J. Chamkha, Chemical reaction on MHD convective heat and mass transfer flow past a rotating vertical cone embedded in a variable porosity regime, Afr. Mat. (2015), 10.1007/s13370-015-0372-1.
11. R. S. Raju, K. Sudhakar, and M. Rangamma, The effects of thermal radiation and Heat source on an unsteady MHD free convection flow past an infinite vertical plate with thermal diffusion and diffusion thermo, J. Inst. Eng. (India): Series C, vol. 94, pp. 175–186, 2013.
12. J. Anand Rao, R. Srinivasa Raju, and S. Sivaiah, Finite Element Solution of heat and mass transfer in MHD Flow of a viscous fluid past a vertical plate under oscillatory suction velocity, J. Appl. Fluid Mech., vol. 5, pp. 1–10, 2012.
13. J. Anand Rao, R. Srinivasa Raju, and S. Sivaiah, Finite Element Solution of MHD transient flow past an impulsively started infinite horizontal porous plate in a rotating fluid with Hall current, J. Appl. Fluid Mech., vol. 5, pp. 105–112, 2012.
14. M. V. Ramana Murthy, R. Srinivasa Raju, and J. Anand Rao, Heat and Mass transfer effects on MHD natural convective flow past an infinite vertical porous plate with thermal radiation and Hall Current, Procedia Eng. J., vol. 127, pp. 1330–1337, 2015.
15. V. S. Rao, L. A. Babu, and R. S. Raju, Finite Element Analysis of Radiation and mass transfer flow past semi–infinite moving vertical plate with viscous dissipation, J. Appl. Fluid Mech., vol. 6, pp. 321–329, 2013.
16. R. Srinivasa Raju, Combined influence of thermal diffusion and diffusion thermo on unsteady hydromagnetic free convective fluid flow past an infinite vertical porous plate in presence of chemical reaction. J. Inst. Engineers (India): Series C, vol. 97, issue 4, pp. 505–515, 2016.
17. K. J. Bathe, Finite Element Procedures, Prentice-Hall, New Jersy, (1996).
18. J. N. Reddy, An Introduction to the Finite Element Method, McGraw-Hill, New York, (1985).